ARTICLE

High-Sensitive Glucose Biosensor Based on Ionic Liquid Doped Polyaniline/Prussian Blue Composite Film

Yao Yao[a], Shou-guo Wu[a*], Hai-hong Xu[b], Li-wen Wang[a]

a. Department of Chemistry, University of Science and Technology of China, Hefei 230026, China
b. Clinical Laboratory, Hefei Third People's Hospital, Hefei 230022, China

(Dated: Received on April 21, 2015; Accepted on September 24, 2015)

The Prussian blue/ionic liquid-polyaniline/multiwall carbon nanotubes (PB/IL-PANI/MWNTs) composite film was fabricated by using cyclic voltammetry. The ion liquid acting as a lubricating agent, could enhance the electron delocalization degree and reduce the structural defects of the polyaniline. The surface morphology of the composite film revealed that the PB nanoparticles have smaller size than that in pure PB film. Due to the introduction of ion liquid, the PB/IL-PANI/MWNTs composite film showed wonderful synergistic effect which can remarkably enhance sensitivity, expand linear range and broaden acidic adaptability for hydrogen peroxide detection. The composite film demonstrated good stability in neutral solution contrast to pure PB film, with a linear range from 2.5 μmol/L to 0.5 mmol/L and a high sensitivity of 736.8 $\mu A\cdot(mmol/L)^{-1}\cdot cm^{-2}$ for H_2O_2 detection. Based on the composite film, an amperometric glucose biosensor was then fabricated by immobilizing glucose oxidase. Under the optimal conditions, the biosensor also exhibits excellent response to glucose with the linear range from 12.5 μmol/L to 1.75 mmol/L and a high sensitivity of 94.79 $\mu A\cdot(mmol/L)^{-1}\cdot cm^{-2}$ for H_2O_2. The detection limit was estimated 1.1 μmol/L. The resulting biosensor was applied to detect the blood sugar in human serum samples without any pretreatment, and the results were comparatively in agreement with the clinical assay.

Key words: Hydrogen peroxide, Prussian blue, Ionic liquid, Glucose biosensor

I. INTRODUCTION

Diabetes is a condition marked by the inability of body to properly manage the level of glucose in the blood, which has become one of the most common health problems nowadays [1]. The diagnosis and control of diabetes mellitus require accurate monitoring of blood glucose [2−4]. Among many types of glucose biosensors, the amperometric enzyme electrodes based on glucose oxidase (GOD) have played a leading role [5]. In terms of the applicability of the biosensors, the enzymes should be immobilized on the electrode to avoid many complications linked to the solution systems. Due to the direct electron transfer between redox centers and electrode surface limited by the three-dimensional structure of enzyme [6, 7], nanostructured materials are being used to immobilize enzymes. It's important to prepare orderly and regular nanostructure which provides high catalytic activity and high surface affinity.

The nanostructured Prussian blue (PB), known as an artificial peroxidase, has been extensively used for H_2O_2 detection and was a fundamental material for possible mass production of glucose biosensors [10−13], due to its excellent catalysis for H_2O_2 reduction at low potentials compared to noble metal, and a relatively cheap and stable electro-catalyst compared to enzyme [10, 13−15]. However, the current response decreases quickly in neutral and alkaline solutions [12]. The operational stability of PB seems to be dependent on the structure regularity of PB film.

Recently, ionic liquids (ILs) [16, 17], which consist entirely of ions, have attracted considerable attention in the field of electrochemistry because of their unique properties such as high conductivity, wide electrochemical window, good thermal stability, and well biocompatibility [18−20]. Many composites to maintain their reactivity require preservation of their highly ordered structures, a condition that is difficult to achieve [21]. ILs are presented as suitable compounds [22, 23]. Therefore, many methods have been attempted to immobilize composites by using ILs combined with carbon nanotubes, hydrogels, nanoparticles, hybrid compounds and other materials of interest [21, 24−30]. Herein, a novel concept is based on using IL to act as lubricating agent in aniline solution, which could enhance the transformation of PANI chains from entanglement state to extend state. In this work, the PB/IL-PANI/MWNTs composite film has been fabricated by electro-deposition step-by-step. The structure and electro-activity of the PB/IL-PANI/MWNTs film were evaluated. The effects

*Author to whom correspondence should be addressed. E-mail: sgwu@ustc.edu.cn

of the volume fraction of IL and the concentration of MWNTs on the formation of the composite film were investigated. The film showed rapid response, good reproducibility, and long-term stability. Furthermore, human serum samples were assayed to demonstrate the practical applicability of this new type of glucose biosensor.

II. EXPERIMENTS

A. Apparatus and reagents

All chemicals from commercial source were of analytical grade. Aniline (≥99.5%) was purchased from Shanghai Chemical Works. The carboxyl multi-walled carbon nanotubes (MWNTs-COOH) were purchased from Nanjing XFNano Material Tech Co. Ltd. Ionic liquid, 1-butyl-methylimidaolium tetrafluorobate ($C_8H_{15}N_2BF_4$, 98%HPLC) was obtained from Shanghai Jiecheng Chemical Co. Ltd. All other chemicals used were purchased from Sinopharm Chemical Reagent Co. Ltd. All solutions were prepared with deionized water. The supporting electrolyte, a fresh phosphate buffer solution (PBS, pH=6.86) was made from K_2HPO_4 and KH_2PO_4.

All electrochemical experiments were carried out on an electrochemical work station (Model LK2010A, LANLIKE Co., Tianjing, China). The three-electrode system consists of the PB/IL-PANNI/MWNTs modified glass carbon electrode (GCE, 3 mm in diameter) as working electrode, a reference electrode (saturated calomel electrode) and a counter electrode (platinum wire). All experiments were performed at room temperature, and high purity nitrogen is used to deaerate the solution if necessary. Scanning electron microscope (SEM) images were obtained on a JEOL JSM-6700F SEM system. pH measurements were performed with a pH meter (Leici Co., Shanghai, China). Ultrasonic cleaning was carried out using an ultrasonic cleaner (40 kHz, Kunshan ultrasonic instrument company, China).

B. Fabrication of the PB/IL-PANNI/MWNTs composite film

Prior to preparation, the GCE was firstly burnished with a fine SiC paper, then polished carefully with aqueous slurries of alumina powder of 1.0, 0.30, and 0.05 μm, successively, and then ultrasonic processed for 3 min in nitric acid (1:1), ethanol and water, respectively, and finally dried with N_2 blowing.

The PB/IL-PANNI/MWNTs composite film was fabricated as follows. First, appropriate amount of carboxyl MWNTs was added into dimethylformamide (DMF) to prepare the suspension solution with MWNTs concentration of 0.1 mg/mL by ultrasonication. Then drop 10 μL MWNTs suspension solution on the well polished GCE and dried in a dryer. The resulting MWNTs/GCE was thoroughly rinsed with water. Second, 750 μL IL was added into 10 mL aqueous solution of 1 mol/L HCl and 0.1 mol/L aniline to prepare the electrolyte. The IL-PANI film was electrochemically deposited on the MWNTs/GCE via cyclic voltammetry by potential cycling between −0.2 and 0.9 V (*vs.* SCE) at a scan rate of 100 mV/s for 15 cycles. After electrodeposition, the IL-PANNI/MWNTs composite film was obtained on the surface of the glassy carbon electrode. Finally, the PB film was also electrochemically deposited on the IL-PANNI/MWNTs/GCE via cyclic voltammetry in the electrolyte containing 2 mmol/L $K_3Fe(CN)_6$, 2 mmol/L $FeCl_3$, 0.1 mol/L KCl and 10 mmol/L HCl, the electrode potential was scanned between −0.2 and 0.6 V for 20 cycles at a scan rate of 50 mV/s. The resulting PB/IL-PANNI/MWNTs/GCE was immediately immersed into a solution containing 0.1 mol/L KCl and 0.1 mol/L HCl, where the electrode potential was scanned between −0.05 and 0.35 V for 30 cycles at a scan rate of 50 mV/s, until a stable voltammetric response was obtained. The electrode surface was then rinsed with deionized water and dried in air.

C. Fabrication of the GOD-CS/PB/IL-PANI/MWNTs biosensor

Chitosan (CS) is a non-acetylated or partially deacetylated chitin. Due to its excellent film-forming ability, biocompatibility, well mechanical strength, cheapness and susceptibility to chemical modifications, it has been widely used for immobilization of enzymes and to fabricate amperometric biosensors. GOD solution was obtained by dissolving 10 mg GOD in 2 mL 0.5% chitosan solution (prepared by dissolving 0.5 g CS in 100 mL 2% acetic acid). Herein, the drop coating method was employed to construct the GOD-CS/PB/IL-MWNTs/MWNTs glucose biosensor. First, taking 10 μL of GOD solution drop onto the PB/IL-PANI/MWNTs/GCE surface carefully, then drying for 60 min at 4 °C in a refrigerator, the enzyme biosensor was accomplished. The enzyme electrode was then kept in a damp condition at 4 °C before use.

III. RESULTS AND DISCUSSION

A. Physicochemical characteristics of the composite films

The morphological images of PB/PANI/MWNTs and PB/IL-PANI/MWNTs film on GCE are illustrated in Fig.1. As can be seen, the actual size and distribution of the PB/IL-PANI/MWNTs film grains is markedly different in comparison with PB/PANI/MWNTs, and the PB/IL-PANI/MWNTs film shows a much denser structure than the PB/PANI/MWNTs. The improvement of the film can be ascribed to IL which is beneficial to

DOI:10.1063/1674-0068/28/cjcp1504058

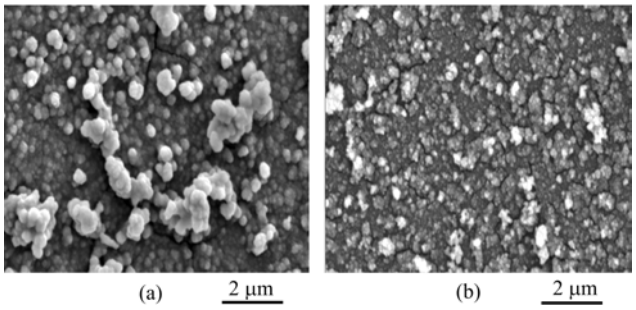

FIG. 1 SEM images of (a) PB/PANI/MWNTs/GCE and (b) PB/IL-PANI/MWNTs/GCE.

the transformation of PANI chains from entanglement state to extend state. The extended PANI chains provide more active centers for PB residing in and growth. On the other hand, IL increase the electron delocalization degree and reduce the structural defects which is conducive to the electrostatic interaction between the positively charged PANI backbone and the negatively charged PB nanoparticles, it is feasible to form a dense robust film in which the content of functional redox centers is higher and extended PANI chains provide more electrostatic binding sites, so that the PB nanoparticles become smaller and uniform.

The electrochemical impedance spectra (EIS) of different electrodes are shown in Fig.2. The diameter of semicircle at higher frequencies in the Nyquist diagram of the impedance spectroscopy represents the interfacial charge transfer resistance (R_{ct}). With the modification of MWNTs onto GCE, the diameter of the semicircle is much smaller than that of bare GCE (Fig.2 (a) and (b)), which suggests that MWNTs greatly improved the electroactivity of the electrode surface. Meanwhile, compared with PANI/MWNTs/GCE, the R_{ct} of IL-PANI/MWNTs/GCE was remarkably decreased (Fig.2 (c) and (d)), indicating that the introduction of IL facilitates heterogeneous electron transfer process. This demonstrates that the electro-activity of IL-PANI/MWNTs composite film is higher than that of PANI/MWNTs.

Linear relationships between peak currents and the square root of the scan rate were obtained from cyclic voltammograms, as shown in Fig.3. The peak currents (both anodic and cathodic) are proportional to the square root of the scan rate. The linear relationships between i_p and $\nu^{1/2}$ were observed in the scan range of 10−250 mV/s (i_{pa}=−0.0576+0.0611$\nu^{1/2}$, R^2=0.9981, i_{pc}=0.0455−0.0416$\nu^{1/2}$, R^2=0.9980), which illustrates that electrode reaction is diffusion controlled.

The stability of the PB nanoparticles was also evaluated by using cyclic voltammetry, according to the decrease of redox peak currents after 150 cycles in different pH solutions. As is shown in Fig.4, the cyclic voltammograms show that the PB/IL-PANI/MWNTs film, contrast to the PB/PANI/MWNTs film and also

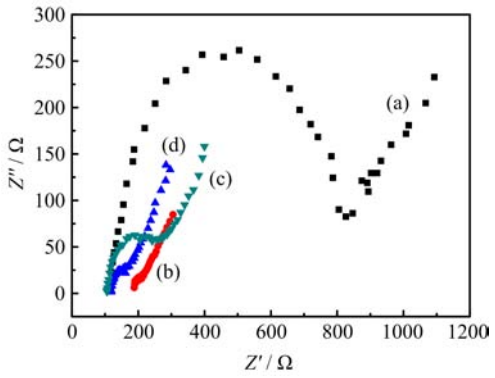

FIG. 2 Nyquist plots of (a) bare GCE, (b) MWNTs/GCE, (c) PANI/MWNTs/GCE and (d) IL-PANI/MWNTs/GCE in 0.1 mol/L KCl containing 10 mmol/L $Fe(CN)_6^{3-/4-}$. The frequency range is from 1 Hz to 100 kHz and the sinusoidal amplitude is 5 mV.

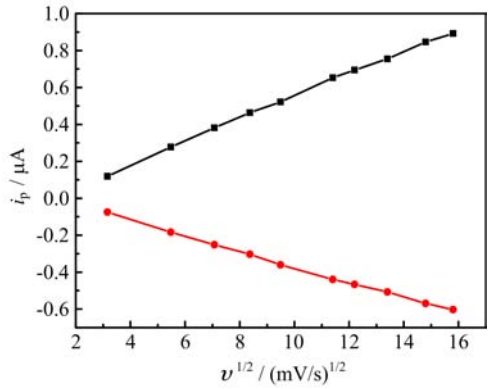

FIG. 3 The plots of peak current (i_{pa}, i_{pc}) *vs.* the square root of the scan rate.

the pure PB film, still retains higher electroactivity after 150 cycles scanning in pH=7.0 solution. The decrease of the peak current does at the level not exceeding 25% even in neutral solution, while the decrease of peak current of PB/PANI/MWNTs film exceeds 50% and pure PB film exceeds 80%. As a base film, the IL-PANI film could improve the stability of PB and keep its electroactivity in neutral even weak alkaline solution. This is because there is a micro acidic environment in the interface between PANI and PB particles, which is provided by the protonation of the nitrogen-containing groups in poly-aniline, it seems to be favorable to stabilization of PB particles, and avoiding decomposition of PB crystals in neutral medium. Furthermore, due to the introduction of IL, the transformation of PANI chains from entanglement state to extend state makes the network structure of PANI more regular, that more protons environment is exposed, which is beneficial to stabilize PB particles.

DOI:10.1063/1674-0068/28/cjcp1504058

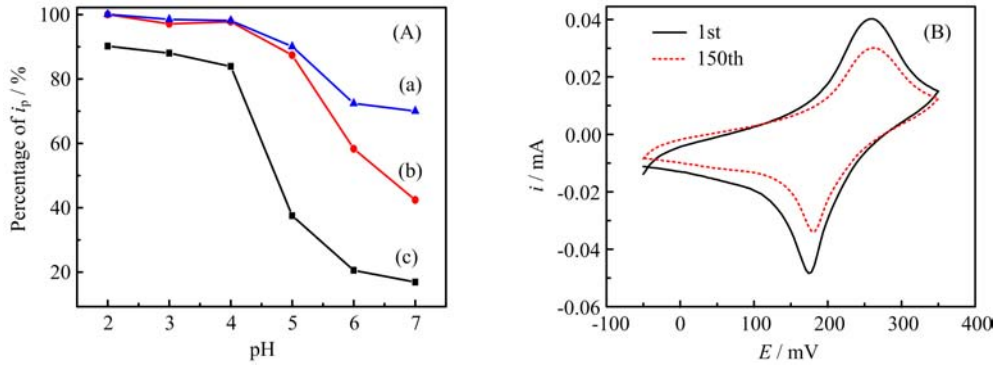

FIG. 4 (A) Electrochemical stability of (a) the PB/IL-PANI/MWNTs film, (b) PB/PANI/MWNTs film and (c) the pure PB film at different pH solutions evaluated from CV peak currents. Conditions: supporting electrolyte, 25 mmol/L PBS+0.1 mol/L KCl with different pH, potential scan rate of 100 mV/s, scan 150 cycles. (B) 1st and the 150th cycle of the CV curves of the PB/IL-PANI/MWNTs film at pH=7.0, respectively.

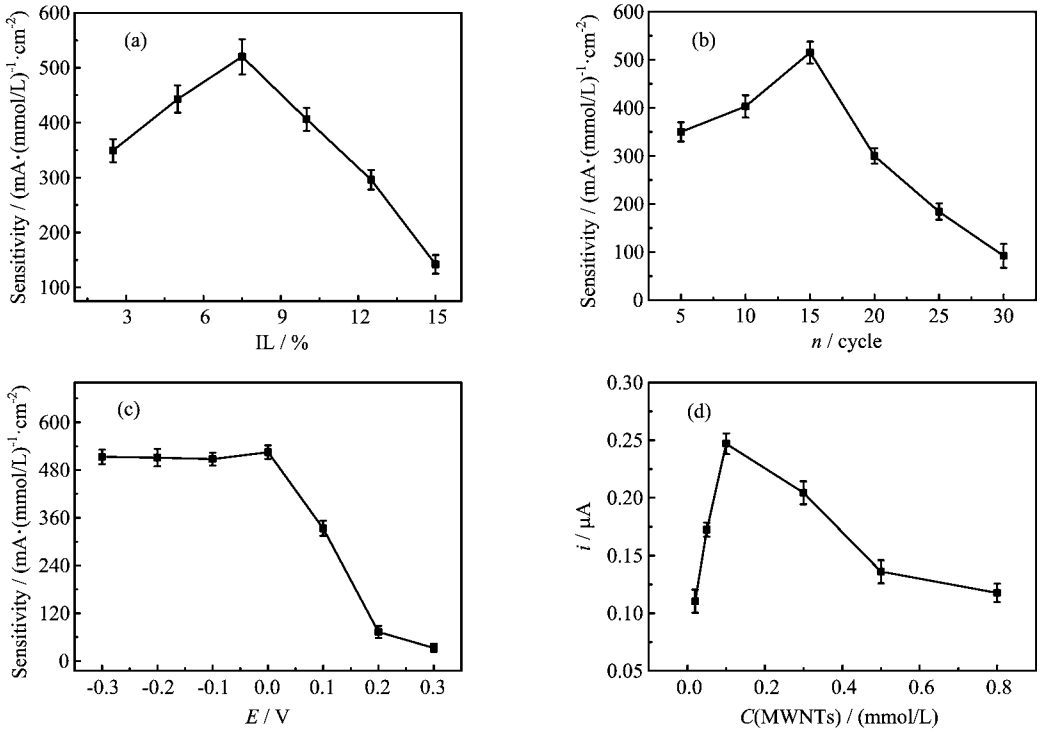

FIG. 5 Dependence of amperometric responses of 0.68 mmol/L H_2O_2 in 0.025 mmol/L PBS at PB/IL-PANI/MWNTs film on (a) the volume fraction of IL, (b) the potential scanning cycles for PB deposition, (c) the working potential, and (d) the concentration of MWNTs.

B. Effect of different factors

The effect of the amount of IL in the aniline solution on the response sensitivity of the composite film was investigated. Experiments were carried out with different IL volume fraction of 2.5%, 5%, 7.5%, 10%, 12.5%, and 15%, respectively. Figure 5(a) gives the amperometric responses and sensitivities of different PB/IL-PANI/MWNTs/GCE towards reduction of hydrogen peroxide. It is obviously that with the volume fraction of IL ranging from 2.5% to 7.5%, the sensitivity increased with the volume fraction of IL increasing regularly, but decreased sharply with the volume fraction beyond 7.5%. Therefore, the volume fraction was chosen as 7.5%.

The potential scanning cycles for PB electrodeposition is another important influencing factor. Obviously the thickness of PB film is increased with the scanning cycles increasing, whereas it influences the current response sensitivity of the composite film. Also the stability (or mechanical stability) of the PB film is affected by its thickness, and then the operability. The thinner

DOI:10.1063/1674-0068/28/cjcp1504058

the PB film is, the faster the current response is and also the higher the sensitivity is, whereas the composite film is less stable. From Fig.5(b), the current response sensitivity of the composite film increased with the potential scanning cycles increasing. While the potential scanning cycles were beyond 15 cycles, the current sensitivity was decreasing gradually. In order to get a relatively good stability and high sensitivity, 15 cycles was selected to prepare the composite film.

As a key parameter, the applied potential at the working electrode is fundamental to achieve the lowest detection limit and to avoid interfering species. From Fig.5(c), the sensitivity of the electrode response increased with the applied potentials ranging from 0.3 V to 0.0 V, then almost unchanged with the applied potential under 0.0 V. Therefore, the applied potential was chosen as 0.0 V, in order to avoid possible interferences in use.

The concentration of MWNTs in the electrolyte influences remarkably on the homogenization which is important to the later deposition. The effect of the concentration of MWNTs on the current response sensitivity was studied in the range from 0.01 mg/mL to 1.0 mg/mL. It can be seen in Fig.5(d) that the current response sensitivity of the composite film increased with the concentration of MWNTs from 0.01 mg/mL to 0.1 mg/mL, and then decreased from 0.1 mL/mg to 1 mL/mg. Herein, 0.1 mL/mg MWNTs was chosen.

C. Amperometric responses of H_2O_2 at the PB/IL-PANI/PB composite film

The cyclic voltammograms, obtained at the PB/IL-PANI/MWNTs composite film respectively in 0.025 mol/L PBS+0.1 mol/L KCl (pH=6.86) solution in absence and in presence of 5 mmol/L H_2O_2, are shown in Fig.6(A). It was observed that the reduction current was increased remarkably due to the electro-catalysis of the Prussian blue towards reduction of H_2O_2.

The electro-catalytic activity of the pure PB film, the PB/PANI/MWNTs film and the PB/IL-PANI/MWNTs film were compared by their amperometric responses through seven times of successive addition of 0.02 mmol/L H_2O_2, as shown in Fig.6(B). Obviously, the response of H_2O_2 at the PB/IL-PANI/MWNTs film is much higher than that at the pure PB film and the PB/PANI/MWNTs film. It is illustrated that the extended PANI chains not only improved the stability of PB particles but also enhanced the current response sensitivity of H_2O_2.

Figure 6(C) shows the amperometric responses of the PB/IL-PANI/MWNTs composite film towards H_2O_2 detection. With the successive addition of H_2O_2 to the solution under gently stirring, the reduction current increased steadily, the response time achieving 95% of the steady-current is less than 1 s. The calibration curve

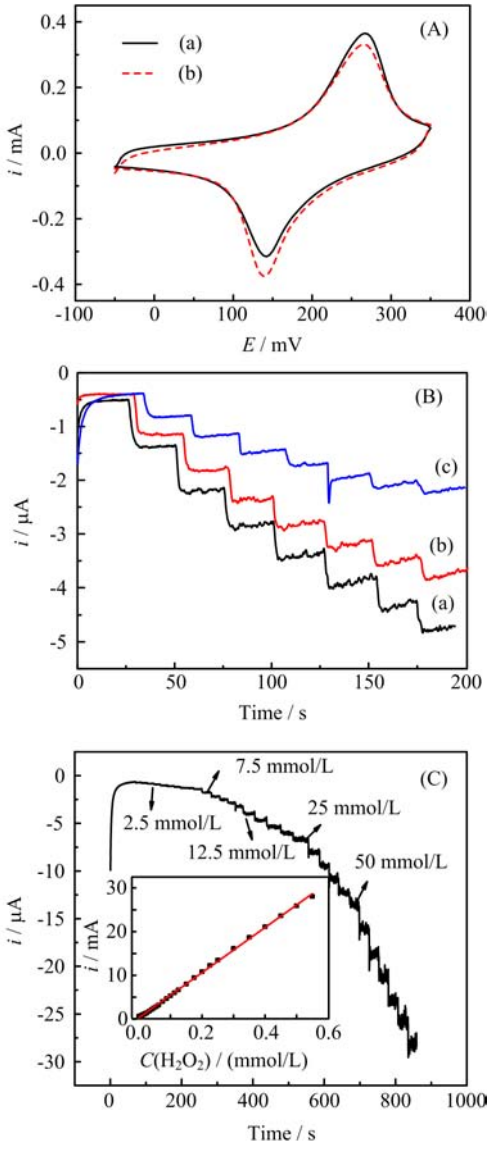

FIG. 6 (A) Cyclic voltammograms of the PB/IL-PANI/MWNTs film in the (a) absence and (b) presence of 5 mmol/L H_2O_2 from −50 mV to 350 mV in 0.025 mmol/L PBS and 0.1 mmol/L KCl at scan rate of 50 mV/s. (B) Amperometric responses of (a) the PB/IL-PANI/MWNTs, (b) the PB/PANI/MWNTs and (c) the PB film to H_2O_2 in 0.025 mmol/L PBS+0.1 mmol/L KCl (pH=6.86) solution. Seven times of successive addition of 0.02 mmol/L H_2O_2, the working potential is 0.0 V. (C) Amperometric response of the PB/IL-PANI/MWNTs film in the concentration of ranging from 2.5 μmol/L to 0.5 mmol/L. The applied potential was 0.00 V. Inset shows the calibration curve of the amperometric response as a function of H_2O_2 concentration.

shows a very wide linearity in the range of 2.5 μmol/L to 0.5 mmol/L with a correlation coefficient of 0.9992. The detection limit was found to be 97.5 nmol/L at signal-to-noise ratio of 3. In particular, the current sensitivity was 736.8 $\mu A\cdot(mmol/L)^{-1}\cdot cm^{-2}$ for H_2O_2. These results indicate that the PB/IL-PANI/MWNTs

DOI:10.1063/1674-0068/28/cjcp1504058

composite film exhibits perfect characteristic for hydrogen peroxide detection.

D. Amperometric detection of glucose using the biosensor based on the GOD-CS/PB/IL-PANI/MWNTs composite film

Considering that chitosan would become insoluble which could be beneficial for the stability of the biosensor when the pH of solution is higher than pK_a (6.3) of chitosan, the buffer solution of pH=6.86 was chosen for the detection of glucose. Figure 7(a) shows the amperometric response of the biosensor to glucose in air-saturated and stirred solution, and the corresponding calibration curve of the biosensor as a function of glucose concentration. The response time required for reaching 95% steady-state current was within 3 s. Figure 7(a) shows the calibration curve of glucose. The enzyme biosensor gave a linear response to glucose in the concentration range from 12.5 μmol/L to 1.75 mmol/L (across two orders of magnitude of glucose concentration) with a correlation coefficient of 0.9926 and the sensitivity was 94.79 μA·(mmol/L)$^{-1}$·cm^{-2} for H_2O_2. And the detection limit of the biosensor was 1.1 μmol/L at signal-to-noise ratio of 3.

Six common electroactive interfering species existing in serum sample, uric acid, ascorbic acid, dopamine, L-histidine, L-cystine and L-cysteine were evaluated. There is no significant change in current response by adding 0.20 mmol/L uric acid (UA), 0.20 mmol/L dopamine (DA), 0.20 mmol/L ascorbic acid (AA), 0.20 mmol/L L-histidine, 0.20 mmol/L L-cysteine and 0.20 mmol/L L-cystine into the test solution containing 0.35 mmol/L glucose, indicating that thus-fabricated biosensor has good anti-interference ability.

In order to illustrate the practical utility of this glucose biosensor, human serum samples were assayed. Fresh serum samples were provided by a local hospital, which were firstly analyzed with the standard clinical assay, *i.e.* glucose dehydrogenase electrode method. As shown in Table I, the test results were in agreement with the data obtained by the clinical assay, and there was no statistically significant difference between these two methods by significance testing (significance level of 0.05). All of these have proved the practical utility of the fast-fabricated biosensor.

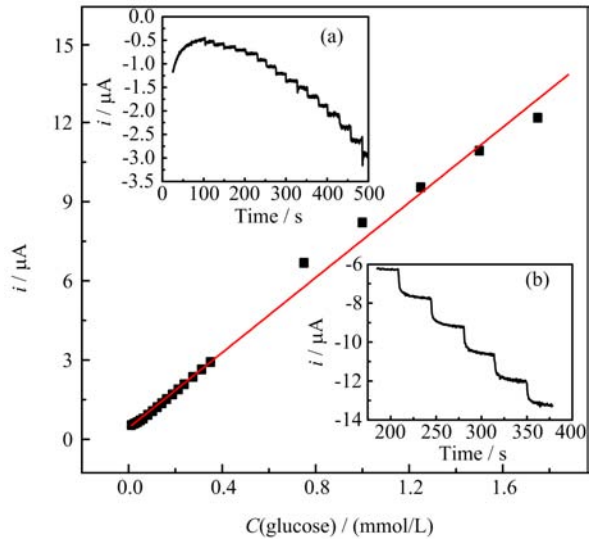

FIG. 7 Calibration curve of the amperometric response of the biosensor as a function of glucose concentration. Inset (a) and (b) give the amperometric response of the biosensor in the concentration of glucose ranging from 12.5 μmol/L to 0.35 mmol/L and 0.75 mmol/L to 1.75 mmol/L respectively. The applied potential was 0.0 V.

TABLE I Glucose test results of the human serum samples.

Sample	Glucose/(mmol/L)		
	Clinical assay	This method[a]	Deviation
1	17.67	17.17	−0.5
2	9.55	9.69	+0.14
3	4.83	4.67	−0.16
4	4.24	4.02	−0.22
5	3.59	3.63	+0.04

[a] The average value of three measurements.

IV. CONCLUSION

We have successfully prepared a new type of glucose biosensor based on the PB/IL-PANI/MWNTs film. The composite film exhibited high sensitivity, fast response, excellent stability and free of interference towards reduction of H_2O_2. The introduction of ionic liquid resultes in a new PANI material, increases the electron delocalization degree, and reduces the structural defects of PANI, which is more effective for PB residing in and growth. On the composite film the PB particles are smaller, and the PB structure is denser. From the excellent performance of the resulting glucose biosensor to glucose detection of the real serum samples, it can be concluded that the ionic liquid doped conducting polymer possesses of potential application in glucose biosensor design and also provides a promising platform for further development of other biosensors.

V. ACKNOWLEDGMENTS

This work was supported by the National Basic Research Program of China (No.933900).

[1] P. Si, Y. Huang, T. Wang, and J. Ma, RSC Adv. **3**, 3487 (2013).

DOI:10.1063/1674-0068/28/cjcp1504058

[2] M. Shamsipur, M. Najafi, and M. R. M. Hosseini, Bioelectrochem. **77**, 120 (2010).
[3] T. Lin, L. Zhong, Z. Song, L. Guo, H. Wu, Q. Guo, Y. Chen, F. Fu, and G. Chen, Biosens. Bioelectron. **62**, 302 (2014).
[4] X. Lv, X. Wang, D. Huang, C. Niu, G. Zeng, and Q. Niu, Talanta **129**, 20 (2014).
[5] S. Wu, G. Liu, P. Li, H. Liu, and H. Xu, Biosens. Bioelectron. **38**, 289 (2012).
[6] Y. Zhang, Y. Li, W. Wu, Y. Jiang, and B. Hu, Biosens. Bioelectron. **60**, 271 (2014).
[7] M. E. Ghica and C. M. A. Brett, Anal. Chim. Acta **532**, 145 (2005).
[8] Y. Zou, L. X. Sun, and F. Xu, Biosens. Bioelectron. **22**, 2669 (2007).
[9] Y. Mu, D. Jia, Y. He, Y. Miao, and H. L. Wu, Biosens. Bioelectron. **26**, 2948 (2011).
[10] L. Liu, L. Shi, Z. Chu, J. Peng, and W. Jin, Sens. Actuat. B **202**, 820 (2014).
[11] S. Ghaderi and M. A. Mehrgardi, Bioelectrochem. **98**, 64 (2014).
[12] L. Zhou, S. Wu, H. Xu, Q. Zhao, Z. Zhang, and Y. Yao, Anal. Methods **6**, 8003 (2014).
[13] F. Ricci and G. Palleschi, Biosens. Bioelectron. **21**, 389 (2005).
[14] N. A. Sitnikova, A. V. Borisova, M. A. Komkova, and A. A. Karyakin, Anal. Chem. **83**, 2359 (2011).
[15] Y. Liu, Z. Chu, and W. Jin, Electrochem. Commun. **11**, 484 (2009).
[16] T. Weith, M. Preiöinger, S. Püllinger, and D. Brüggemann, Heat Trans. Engin. **35**, 1462 (2014).
[17] Z. Wang, F. Li, J. Xia, L. Xia, F. Zhang, S. Bi, G. Shi, Y. Xia, J. Liu, Y. Li, and L. Xia, Biosens. Bioelectron. **61**, 391 (2014).
[18] W. Zhilei, L. Zaijun, S. Xiulan, F. Yinjun, and L. Junkang, Biosens. Bioelectron. **25**, 1434 (2010).
[19] Y. Zhang, Y. Liu, Z. Chu, L. Shi, and W. Jin, Sens. Actuat. B **176**, 978 (2013).
[20] A. N. Tran, T. N. Van Do, L. P. M. Le, and T. N. Le, J. Fluorine Chem. **164**, 38 (2014).
[21] K. S. Galhardo, R. M. Torresi, and S. I. C. de Torresi, Electrochim. Acta **73**, 123 (2012).
[22] J. F. B. Pereira, R. Costa, N. Foios, and J. A. P. Coutinho, Fuel **134**, 196 (2014).
[23] S. Menne, M. Schroeder, T. Vogl, and A. Balducci, J. Power Sources **266**, 208 (2014).
[24] Y. Zhang and J. Zheng, Electrochim. Acta **54**, 749 (2008).
[25] R. Gao and J. Zheng, Electrochem. Commun. **11**, 608 (2009).
[26] J. Lin, C. He, Y. Zhao, and S. Zhang, Sens. Actuat. B. **137**, 768 (2009).
[27] X. Zeng, X. Li, L. Xing, X. Liu, S. Luo, W. Wei, B. Kong, and Y. Li, Biosens. Bioelectron. **24**, 2898 (2009).
[28] X. Shangguan, H. Zhang, and J. Zheng, Electrochem. Commun. **10**, 1140 (2008).
[29] A. Safavi, N. Maleki, and E. Farjami, Biosens. Bioelectron. **24**, 1655 (2009).
[30] M. C. Tsai and Y. C. Tsai, Sens. Actuat. B **141**, 592 (2009).

DOI:10.1063/1674-0068/28/cjcp1504058